1996 Conference on Composites, Advanced Ceramics, Materials and Structures, American Ceramic Society, Cocoa Beach, FL, January 1996, to be published in Ceramic Engineering and Science Proceedings

P96-02

MULLITE FIBER REINFORCED REACTION BONDED Si_3N_4 COMPOSITES

T. Saleh, A. Lightfoot and J. Haggerty
Massachusetts Institute of Technology
Cambridge, MA 02139

A. Sayir
NASA Lewis Research Center
Cleveland, OH 44135

INTRODUCTION

Fracture toughnesses of brittle ceramic materials have been improved by introducing reinforcements and carefully tailored interface layers. Silicon carbide and Si_3N_4 have been emphasized as matrices of structural composites intended for high temperature service because they combine excellent mechanical, chemical, thermal and physical properties. Both matrices have been successfully toughened with SiC fibers, whiskers and particles for ceramic matrix composite (CMC) parts made by sintering, hot pressing or reaction forming processes.

These SiC reinforced CMCs have exhibited significantly improved toughnesses at low and intermediate temperature levels, as well as retention of properties at high temperatures for selected exposures; however, they are vulnerable to attack from elevated temperature dry and wet oxidizing atmospheres after the matrix has cracked. Property degradation results from oxidation of interface layers and/or reinforcements.[1] The problem is particularly acute for small diameter (~20 μm) polymer derived SiC fibers used for weavable toes.

This research explored opportunities for reinforcing Si_3N_4 matrices with fibers having improved environmental stability; the findings should also be applicable to SiC matrix CMCs. High purity reaction formed Si_3N_4 (RBSN) was selected as the matrix because, like CVI-SiC, it yields a phase-pure matrix (ideally containing only a mixture of α- and β- polytype Si_3N_4 or SiC) needed for high temperature mechanical properties by a net-size process which avoids stresses induced by shrinkage around dimensionally stable reinforcements. Single-phase single-crystal mullite fibers were selected as a reinforcement because this material combines an appropriate coefficient of thermal expansion (CTE) (Figure 1)[2,3] and oxidation resistance with excellent high temperature properties. The single-phase mullite is not degraded by nitridation temperatures and atmospheres; also, single crystals have exhibited excellent strength retention (80% of room temperature values of 1.15 GPa) to 1400°C.[4] The CTE values in Figure 1 indicate a tendency for the mullite fibers to pull away from the matrix when cooled from processing temperatures, thereby forming the gaps of the type sought with fugitive coatings. These exploratory experiments did not employ interface layers between the fibers and matrix phases.

19960222 047

DISTRIBUTION STATEMENT A
Approved for public release;
Distribution Unlimited

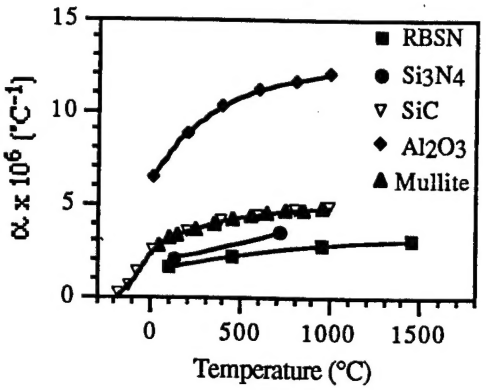

Figure 1. Coefficients of thermal expansion for RBSN, polycrystalline mullite and other important materials.[2,3]

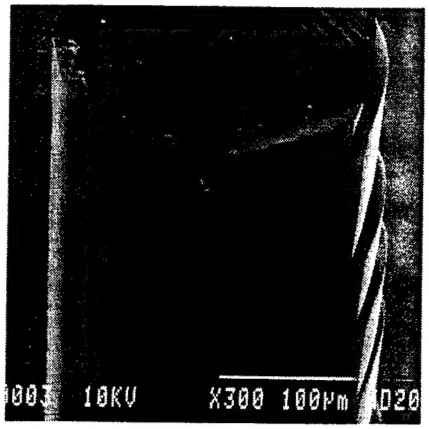

Figure 2. As-grown single crystal mullite fiber which exhibits characteristic stepped facets.

APPROACH AND PROCEDURES

The viability of reinforcing low thermal expansion coefficient, non-oxide matrices with oxide fibers was assessed by the following observations and characterizations. Disk-shaped composites with a single layer of aligned fibers (positioned ~1/4 through the thickness) were broken in a 3 point bend fixture so that the fibers were aligned with and subject to primarily tensile stresses. Fiber pull-outs and exposed fiber-matrix interfaces were characterized by microscopy. Fiber-to-matrix bonding was measured by push-out tests and by a single fiber microcomposite tensile test. Finally, the effect of mullite fibers on the nitriding kinetics of high purity Si powder was determined by thermogravimetric analysis (TGA) and by phase analysis using quantitative X-ray diffraction (XRD). Interfaces exposed by breaking a sample after TGA were also examined by microscopy.

The majority of the fibers used for this research were single-phase single crystals (diameter: ~ 200 - 300 µm) grown by the laser heated floating zone process[4-7] at the NASA-Lewis Research Center. The compositions of the single crystals are between the $2SiO_2 \cdot Al_2O_3$ and $3SiO_2 \cdot 2Al_2O_3$ limits. A few composite samples used for pullout length and interface characterizations were also made either with melt grown fibers containing two phases that were aligned parallel to the growth axis or with polycrystalline sintered mullite-alumina fibers (Nextel 720 produced by 3M Co.). Fibers were broken to length and cleaned in soap and water, acetone and isopropanol ultrasonic baths prior to use in composites. Some fiber was provided imbedded in epoxy and was removed by heating in air prior to cleaning. The epoxy char was easily removed.

High purity, submicron (~0.2-0.3 µm) SiH_4 derived Si powder was used to synthesize the RBSN matrices in investigated samples.[8] For aligned fiber composites, the Si powder was dispersed and colloidally pressed, incorporating 1.5 wt.% polystyrene as a binder, into 1.27 cm diameter disks as described previously.[9] A disk having a thickness equal to 1/4 the final desired thickness was pressed, 5-10 mullite fibers were placed parallel to one another and separated by 2-4 diameters on the Si disk, the disk and fibers were replaced into the die, and then the fibers were encapsulated by colloidally pressing the remaining thickness of the disk. In some cases, colloidally pressed samples were densified further by warm isopressing (temperature: 110°C, pressure: 275 MPa).

Single fiber, microcomposite samples were made by dip coating individual 7.6 cm long single crystal mullite fibers in a xylene slip containing 10 vol% Si and 6.5 vol% total additives (monocarboxypolystyrene, polyvinylbutyral and benzylbutyl-phthalate). The coating thickness and fiber diameter of a fractured sample indicate an average thickness increase of ~10 μm per dip. Using the total weight gain, coating thickness and theoretical dried slip density of 1.79 g/cc, the nitrided coating density is calculated to be ~35%. This is less than half the typical colloidally pressed, nitrided density of ~75%. One microcomposite sample was subjected to a tensile test, as described elsewhere.[10]

Samples were nitrided in flowing UHP nitrogen following procedures typical for nitriding of this high purity Si which has been shaped with binders.[8,11] Initial heating rates were 2-3°C/min with 12 hr holds at 1225°C, and continued at 0.5°C/min to 1380°C which was held for 10 hrs.

Samples used for push out measurements of bond strength were made by cutting 680 to 720 μm thick slices oriented perpendicular to the fiber axes. Sample surfaces were polished down to 3.0 μm diamond. Bond strength measurements were made using the technique described by Marshall[12] and apparatus fitted with tungsten carbide punches described previously.[13] The load displacement data were collected with a computer and the experiment was monitored with a video camera. The interfacial shear strength (τ_s) is determined by measuring the applied force (F) needed to debond the fibers and initiate sliding, the fiber length (specimen thickness t), and fiber diameter (d). The interfacial shear stress (τ_s) is equal to $F/(\pi dt)$.

Dry pressed samples were used to determine the effect of mullite on the silicon nitriding kinetics.[14] This eliminates effects of binder and solvent exposures and allows fast heating rates (100°C/min) which minimize effects of any impurities in the nitriding atmosphere. These samples were nitrided at 1250°C because prior research has determined that the effects on reaction kinetics are particularly evident at this temperature.

Environmental and field-emission scanning electron microscopes were used to characterize surfaces in the CMC looking for any evidence of interactions between the fibers and matrix that might be responsible for chemical bonding between them, or for degradation of the fibers during processing. Both of these microscopes permit high magnification imaging (up to 28,500 X) of insulating materials without employing conductive coatings.

RESULTS & DISCUSSION

Mullite Fibers

Figure 2 shows a typical as-grown single crystal mullite. Distortion from an ideal cylindrical shape by both flat and stepped surface facets was typical of the single crystal fibers used in this research. TEM analysis shows that the fibers grow in a direction that is close to the c-axis of the rhombohedral lattice, and that the facet surfaces correspond to {110} type planes.[4] The spacing distance, the regularity and the amplitude of facet steps varied considerably between individual fibers and sometimes along the lengths of individual fibers. Axial steps were also observed at transitions between adjacent facet planes.

Usually fracture origins could be traced[4] to the steps like those that are evident in Figure 2. Sharply intersecting planes evidently weaken the fibers due to localized stress concentrations. Also, it should be anticipated that the stepped facets will physically inhibit fibers from sliding.

Improved strengths and reinforcing action requires either suppressing facet formation or causing facets to form in a plane containing the growth axis, thereby eliminating the steps. The latter approach has been used successfully to eliminate facet steps on both a-axis sapphire and spinel ($MgO{\cdot}Al_2O_3$) fibers;[15] however, growth from precisely oriented [001] seeds hasn't yet been pursued with mullite fibers. Polycrystalline mullite fibers grown by the laser heated floating zone process were free of these facets, and approached ideal cylindrical shapes.

Interfacial Shear Strength

After exhibiting a few small discontinuities in their load-displacement curves, single crystal mullite fibers slipped discontinuously at loads between 30 to 40 N for the combination of the fiber diameters (230 to 300 μm) and lengths (680 to 720 mm) used in these push-out test specimens. Two representative load-displacement curves are shown in Figure 3. Fiber slippage was not apparent in the TV images at the points where small discontinuities were observed. The interfacial shear strengths for the first major load drop correspond to approximately 60 MPa.

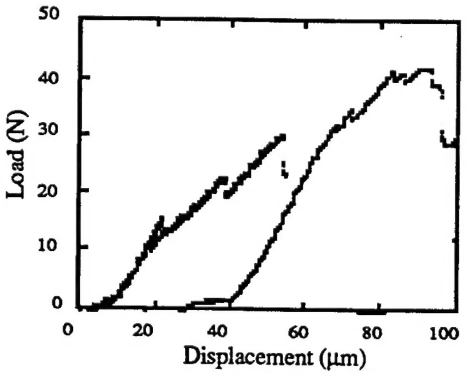

Figure 3. Two typical load-displacement traces for fiber push-out tests. Initial displacement is arbitrary.

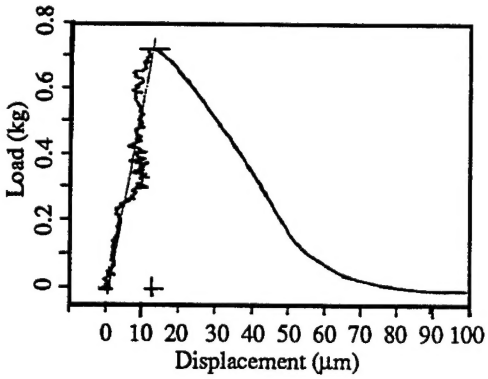

Figure 4. Load-displacement trace for single fiber microcomposite tensile test.

Frequently the tungsten carbide anvils and/or the fibers fractured at the high loads required to push these large diameter fibers out of the matrix, making interpretation of the results somewhat ambiguous. In all of the well behaved tests, slippage was accompanied by significant drop in load level. This characteristic indicates that slippage occurred when fiber-to-matrix bonds failed, or when a physical irregularity was forced through a barrier. Upon slippage, most experimental loads dropped to levels that were still significant, then increased with approximately the same slope as the loading anvil was advanced. The combination of the observed load-displacement traces and the stepped facets on the fibers strongly suggests that slippage is inhibited by interfacial friction resulting from physical interference.

Figure 4 shows the load-displacement curve observed for the microcomposite tensile sample shown in Figure 5. After the fiber failed at a tensile load of 7.2 N, the load decreased smoothly as the protruding end of the fiber was extracted from the RBSN sheath. Although the wedge shape of the protrusion makes precise calculations difficult, the interfacial shear strength can be estimated assuming that relative motion was resisted as long as the cord length of the fully extracted portion of the fiber remained less than 1-diameter. The micrograph in Figure 5 shows that the fiber began

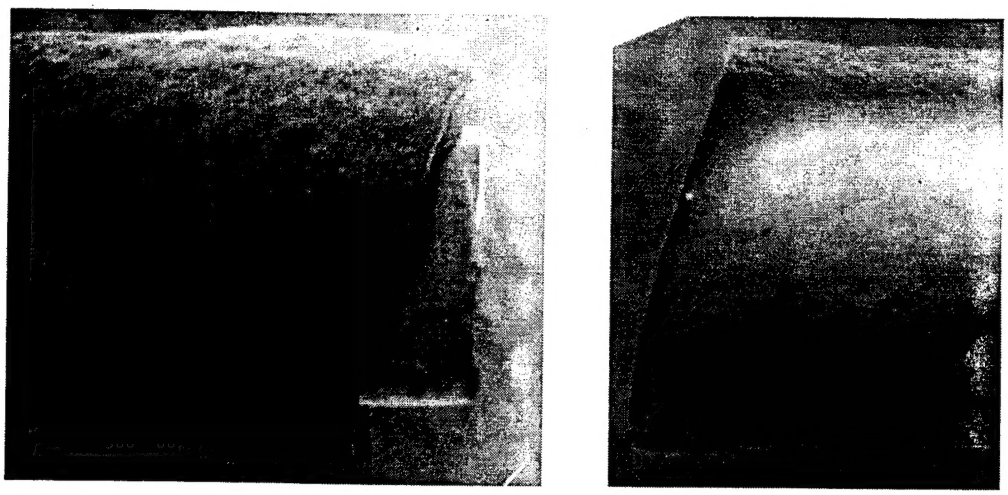

Figure 5. Sample after single fiber microcomposite tensile test. Fiber diameter is 201 μm.

to pull clear of the sheath when extracted 20 μm, and was completely separated when extracted 100 μm. As observed in Figure 4, the load reached zero at ~70 μm extraction corresponding to the point where the cord length just reached 1-diameter and the fiber was no longer radially constrained. Using the observed dimensions and load, the shear stress required to induce slippage between the fiber and the matrix is approximately 190 MPa.

Unlike the push-out results, the microcomposite tensile test did not exhibit a sudden drop in load when slippage commenced. Microscopy of the protruding fiber and exposed sheath showed that this short section of fiber (slippage length < 0.5 diameter) had 2 facet steps in the vicinity of the failure; one coincided with the location where the fiber broke and the other where the matrix sheath fractured. Unlike the facet steps that are suspected of impeding slippage in the push-out measurements (slippage length ≈ 3 diameters), the orientations of these facet steps did not interfere with slippage in the tensile test.

With the simplifications used in the calculations and the limited number of test samples, there is little basis for making quantitative comparisons between the interfacial shear strength values observed with the push-out and microcomposite tensile measurement techniques. Qualitatively, the two measurements do indicate that there is little, if any, bonding between single crystal mullite fibers and a RBSN matrix. Also, the shear strength levels are in an appropriate range to expect composite behavior.[16]

Microscopy of Surfaces and Interfaces

Figure 6 shows portions of two flat facet surfaces, a facet step between the two, and an adjacent smooth curved surface on an as-grown single crystal mullite fiber like the stepped surfaces in Figure 2. All of these surfaces except for the facet step exhibit a uniformly distributed submicron hemispherical feature that has not been observed previously on fibers of the many materials that have been grown by this process. Similar features having larger dimensions were also evident at lower levels of magnification. Generally it appears that the features protrude outward (convex). Neither the nature of these unusual features nor their cause has been identified. It was observed that mullite fiber growth is accompanied by an unusual and vigorous evolution of bubbles on the

melt surface. These features could result directly from entrapped bubbles, indirectly from debris spattered from bursting bubbles, or could be condensed from SiO_2 that is vaporized from the melt during growth. While generally present, these bumpy surfaces were not evident on all surfaces of every fiber, and other less common features were also observed.

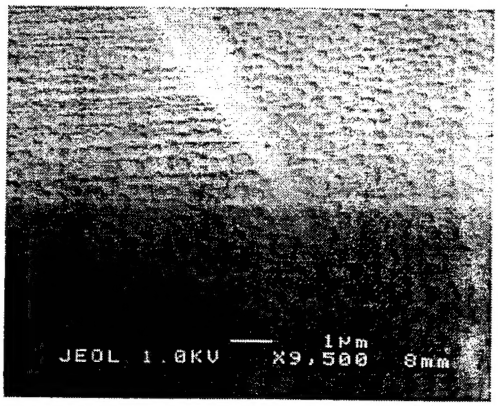

Figure 6. Surface of as-grown single crystal mullite fiber, observed on uncoated sample with FESEM, showing that small scale bumps were present before exposure to nitriding process.

Figure 7 shows a mullite fiber surface that was exposed by fracturing a mullite-RBSN sample used for investigating nitriding rates. This fiber exhibits the same uniformly distributed submicron feature observed on the as-grown fibers which appear unaffected by the Si nitriding process. Particulate debris is found on a small fraction of the mullite fiber surface within nitrided samples. The submicron equiaxed features have the same size and shape as the nitride particles making up the RBSN matrix. They are sufficiently bonded to the fiber surfaces that they cannot be removed with a tetrafluoroethane jet. Also evident are widely dispersed, small rod-shaped particles. Based on previous observations,[14] it is believed that these are α-Si_3N_4 particles formed in the gas phase in the presence of oxygen contamination. These results show that fiber surfaces are minimally impacted by exposures encountered during incorporation into the matrix as well as the reaction bonding process.

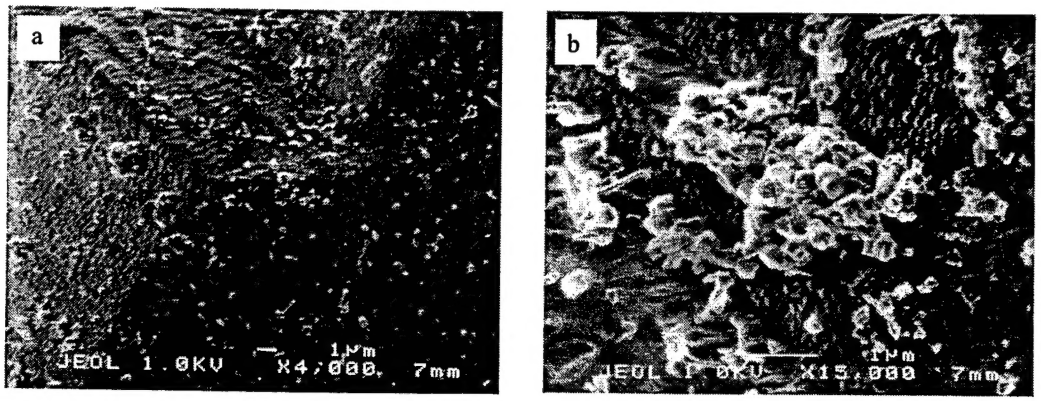

Figure 7. (a) Surface of single crystal mullite fiber in vicinity of facet step after exposure to nitriding conditions. A low concentration of spherical and rod-shaped debris is shown. (b) Higher magnification of a facet step adjacent to the one shown in 7a. Spherical debris is RBSN grains from matrix; rods are probably α-Si_3N_4 particles. Small scale bumps observed in Figure 6 are evident.

Interfaces between fibers and matrices usually appeared slightly separated. When cooled from 1400°C, a radial gap of $\approx$ 0.3 μm is predicted for 200 μm diameter fibers based on the CTE

differential shown in Figure 1. It should be noted that these CTEs may not exactly represent the materials used because single crystal mullite exhibits anisotropic CTEs that differ from the polycrystalline values shown in Figure 1, and also, the RBSN value corresponds to a different grade of RBSN. Acknowledging these potential errors, it is unlikely that differential CTE could make the gap larger than ≈ 1 μm. Thus, physical interference with slippage should be expected because all of the mullite fibers had surface irregularities with greater amplitudes.

Nitriding Kinetics

TGA results for a reference Si sample and a sample made from a mixture of 93.5 wt% Si and 6.5 wt% mullite (chopped single crystal fibers) were nearly identical when normalized to their Si contents. The beginning of the induction period weight-gains were observed at ~850°C and rapid reactions commenced between 1100 and 1200°C. The extents of conversion by weight gain were both 96%; one sample was confirmed by XRD to be 98.3%. All values are typical of dry pressed SiH_4 derived Si powders nitrided to a maximum temperature of 1250°C.[17]

The matrix surfaces exposed where fibers were pulled out of these 1250°C samples exhibited a thin layer (~ 10 μm) having the brown color normally exhibited by incompletely nitrided Si powder. The push-out samples, nitrided to 1385°C, did not exhibit discoloration at the fiber-matrix interfaces. The limited and localized inhibition of the nitriding reaction observed at 1250°C is eliminated at normal nitriding temperature levels.

CONCLUSIONS

These exploratory experiments have successfully demonstrated features that are essential for high temperature ceramic matrix composites. Uncoated single crystal mullite fibers can be incorporated into a high purity RBSN matrix without damaging either the fiber or matrix phases and without significantly inhibiting nitriding kinetics. Pull-out lengths observed for flexural and tensile samples show that fibers slide relative to the matrix phase during fracture. The load-displacement traces observed for interfacial shear strength measurements and microscopy results both indicate that there is little if any chemical bonding between the fibers and matrices. Resistance to sliding probably arises primarily from mechanical interference caused by shape irregularities. Thus, mullite fibers having more uniform radii, either by eliminating or controlling the orientations of surface facets, should exhibit somewhat lower interfacial shear strengths than the measured values (60 and 190 MPa). Interface shear strength levels for uncoated fibers are within an appropriate range for producing tough composites with these constituent materials. Use of interface layers would provide an opportunity for modifying and controlling interface shear strengths, but would be accompanied with well known complexity, cost and vulnerability issues. Overall, these experimental results demonstrate an uninvestigated opportunity for robust, high temperature ceramic matrix composites based on reaction formed Si_3N_4 or SiC matrices.

REFERENCES

1. N. Okabe, I. Murakami, H. Hirata, Y. Yoshioka and H. Ichikawa, "Environmental Deterioration and Damage of Ceramic Matrix Composites," Ceram. Eng. Sci. Proc. **16** [5] 885-892 (1995).
2. A.J. Moulson, "Review – Reaction-Bonded Silicon Nitride: its Formation and Properties," J. Mater. Sci., **14**, 1017-51 (1979).
3. W.D. Kingery, H.K. Bowen and D.R. Uhlmann, Introduction to Ceramics, John Wiley & Sons, 1976, p. 593.

4. A. Sayir and S. Farmer, "Directionally Solidified Mullite Fibers," in Ceramic Matrix Composites-Advanced High-Temperature Structural Materials, eds., R.A. Lowden, M.K. Ferber, J.R. Hellman, K.K. Chawla and S.G. DiPietro, Mat. Res. Soc. Symp. Proc., 365, 11-21 (1995).
5. J.S. Haggerty and W.P. Menashi, "Production of Oxide Fibers by a Floating Zone Fiber Drawing Technique," NASA, Contract No. NAS 3-13479, Feb 1971.
6. J.S. Haggerty, W.P. Menashi and J.F. Wenckus, Method for Forming Refractory Fibers by Laser Energy, USP 3,944,640, Mar 16, 1976.
7. J.S. Haggerty, W.P. Menashi and J.F. Wenckus, Apparatus for Forming Refractory Fibers, USP 4,012,213, Mar 15, 1977.
8. J.S. Haggerty, "Synthesis and Properties of Reaction Bonded Silicon Nitride made from High Purity Si Powders," in Ceramic Transactions, Vol. 42, Silicon-Based Structural Ceramics, eds. Brian W. Sheldon and Stephen C. Danforth, American Ceramic Society, Westerville, OH, pp. 29-45.
9. T.A. Saleh, "Reaction Bonded Silicon Nitride Composites with Mullite Fibers," S.B. Thesis, Massachusetts Institute of Technology, Materials Science and Engineering, June 1995.
10. G.N. Morscher, J. Martinez-Fernandez, and M.J. Prudy, "Determination of Interfacial Properties Using a Single Fiber Microcomposite Test," NASA HI-TEMP Review, Cleveland, OH, Publication 10146 pp. 77-1 to 77-10.
11. "Reaction Bonded Silicon Nitride for Endoatmospheric Hypersonic Radome Technology," Interim Final Report, Contract No.: DASG 60-91-C-0124, August 1, 1993.
12. D.B. Marshall and A.G. Evans, "Failure Mechanisms in Ceramic-Fiber Ceramic-Matrix Composites, "J. Am Ceram Soc., **68** [5] 225-231 (1985).
13. J. I. Eldridge, "Desktop Fiber Push-Out Apparatus," NASA TM 105341, [12] 1991.
14. A. Lightfoot, B.W. Sheldon, J.H. Flint, and J.S. Haggerty, "Nitriding Kinetics of Si-SiC Powder Mixtures as Simulations of Reaction Bonded Si_3N_4-SiC Composites," Ceram. Eng. Sci. Proc. **10** [9-10] 1035-48 (1989).
15. J.E. Sheehan, J. Sigalovsky, J.S. Haggerty, and J.R. Porter, "Mechanical Properties of $MgAl_2O_4$ Single Crystal Fibers," Ceram. Eng. Sci. Proc. **14** [7-8] 660-670 (1993).
16. J.I. Eldridge and R.T. Bhatt, "Experimental Investigation of Interface Properties in SiC Fiber Reinforced Reaction-Bonded Silicon Nitride Matrix Composites," in Ceramic Matrix Composites-Advanced High-Temperature Structural Materials, eds., R.A. Lowden, M.K. Ferber, J.R. Hellman, K.K. Chawla and S.G. DiPietro, Mat. Res. Soc. Symp. Proc., 365, 353-364 (1995).
17. B.W. Sheldon, "The Formation of Reaction Bonded Silicon Nitride from Silane Derived Silicon Powders," Sc.D. Thesis, Massachusetts Institute of Technology, Materials Science and Engineering, January 1989.

ACKNOWLEDGMENTS

This research was supported at MIT by ONR under contract No. N00014-94-1-0425 and by in kind support at NASA Lewis Research Center. These contributions are gratefully acknowledged.